Journal of Thermal Analysis and Calorimetry
https://doi.org/10.1007/s10973-019-08564-3

Investigation of convective nanomaterial flow and exergy drop considering CVFEM within a porous tank

Abdulrahman A. Alrobaian[1] · Ali Sulaiman Alsagri[2] · Jagar A. Ali[3,4] · Samir Mustafa Hamad[5,6] · Ahmad Shafee[7,8] · Truong Khang Nguyen[7,8] · Zhixiong Li[9,10]

Received: 15 February 2019 / Accepted: 4 July 2019

Abstract

In the current research, ferrofluid migration and exergy destroyed became the main goal. Demonstration of characteristics impact of permeability, buoyancy and Hartmann numbers on variation of nanomaterial movement as well as irreversibility was examined. CVFEM with triangular element is utilized to calculate the solution of formulated equations. An increment in magnetic field results in greater exergy drop which is not beneficial in view of convective mode. An increase in permeability demonstrates a growth of nanomaterial convective flow. Augmenting *Da* causes a reduction in Bejan number while it makes Nu_{ave} to augment.

Keywords Magnetic force · Convective · Porous space · Nanofluid · Entropy

Introduction

Nanofluid can be offered as an efficient carrier fluid because of its capability to enhance thermal feature [1–8]. Two important issues including extra stream resistance and possible erosion should not be ignored because the particles are not stable in the suspension phase. For these reasons, there has not any effort to commercialize such fluids including particles which are interspersed and coarse-grained [9–17]. Modern nanotechnology gives us the opportunity to generate and to process substances including crystallite scale which are less than 50 nm. General definition of nanofluid is fluids with suspended nanoparticles [17–20]. Therefore, basis fluids flowing with certain heat transfer features can pursue different patterns of behavior when nanoparticles are suspended in them [21–24]. Several new techniques were suggested to augment performance [25–31]. Mixture of H_2O and MWCNT was employed by Hussien et al. [32] within a mini duct, and friction factor was analyzed numerically. They reported Nu improvement as a consequence of dispersing nanomaterial.

Multi-louvered fins have been mounted by Kumar et al. [33] inside a duct filled with alumina. Performance of unit augmented about 80% with 0.2% nanomaterial fraction. Wu et al. [34] employed copper powder to expedite the charging of paraffin and reported 32% reduction in melting

✉ Ahmad Shafee
babac99@hotmail.com; ahmad.shafee@tdtu.edu.vn

1 Mechanical Engineering Department, College of Engineering, Qassim University, Buraydah, Saudi Arabia

2 Mechanical Engineering Department, College of Engineering - Unaizah, Qassim University, Unaizah, Saudi Arabia

3 Department of Petroleum Engineering, Faculty of Engineering, Soran University, Soran, Kurdistan Region, Iraq

4 Department of Petroleum Engineering, College of Engineering, Knowledge University, Erbil, Kurdistan Region, Iraq

5 Computer Department, Cihan University-Erbil, Erbil, Saudi Arabia

6 Scientific Research Centre, Soran University, Soran, Kurdistan Region, Iraq

7 Division of Computational Physics, Institute for Computational Science, Ton Duc Thang University, Ho Chi Minh City, Vietnam

8 Faculty of Electrical and Electronics Engineering, Ton Duc Thang University, Ho Chi Minh City, Vietnam

9 School of Engineering, Ocean University of China, Qingdao 266110, China

10 School of Mechanical, Materials, Mechatronic and Biomedical Engineering, University of Wollongong, Wollongong, NSW 2522, Australia

Published online: 26 July 2019

time for 1% fraction. Variable magnetic impact for controlling forced convection was investigated by Mehrez and Cafsi [35], and they concluded that impact of nanoparticles fraction is function of Hartmann number. There exist various passive ways for augmentation of efficiency like inserting fins, etc. [36–47]. Beryllium oxide has been mixed with deionized water by Selvaraj et al. [48] to generate new carrier fluid for saving energy. TiO_2 nanomaterial for cooling of sinusoidal duct was employed by Sajid et al. [49], and they achieved the highest performance with 0.012% fraction of powder. Among various numerical approaches which are offered by various researchers [50–85], there is very accurate method which combined two powerful approaches and its name is CVFEM which was employed in various applications [86–100] and proved the high power of this technique. As mentioned in [101], CNT nanoparticles can be utilized corrugated cavity in existence of rotational heat source inside the domain. They showed that geometric variable has greater impact than fraction of nanomaterial. Parabolic collector performance was analyzed by Bellos and Tzivanidis [102]. They tried to improve the efficiency with mounting fins and dispersing CuO.

In this article, variations of entropy of nanomaterial by imposing Lorentz forces were illustrated. Behaviors of nanofluid through a permeable media were examined. CVFEM was utilized to illustrate the impacts *Da*, *Ra* and *Ha*.

Geometry and mathematical model

A permeable tank with circular hot inner cylinder is illustrated in Fig. 1. The testing fluid is iron oxide–water nanomaterial. To inform about the amount of properties of nanomaterial components, Ref. [103] can be reviewed. It should be noticed that formulation for nanomaterial is as same as that paper, too. The outer wall is maintained at T_c, and domain was affected by magnetic effect in one direction. For macroscopic simulation, non-Darcy law was involved with considering single-phase model. To gain the accurate solution, we utilized CVFEM which was suggested by Sheikholeslami [104] in last seven years. He combined the benefits of FVM and FEM to achieve more accurate approach. The formulations for our model are:

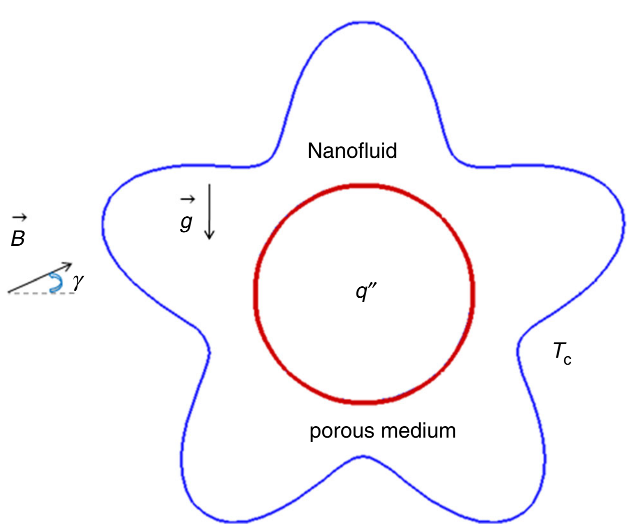

Fig. 1 Related domain of the current article

$$\frac{\partial v}{\partial y} + \frac{\partial u}{\partial x} = 0 \tag{1}$$

$$\begin{aligned}&(\rho_{nf})\left(\frac{\partial u}{\partial y} v + u\frac{\partial u}{\partial x}\right) = \\ &\quad\left[+\sigma_{nf} B_x B_y v - \sigma_{nf} B_y^2 u + \left(\frac{\partial^2 u}{\partial y^2} + \frac{\partial^2 u}{\partial x^2}\right)\mu_{nf} - \frac{\partial P}{\partial x} - \frac{\mu_{nf}}{K} u\right],\\ &(B_y, B_x) = B_o(\sin\gamma, \cos\gamma)\end{aligned} \tag{2}$$

$$\begin{aligned}&\rho_{nf}\left(v\frac{\partial v}{\partial y} + \frac{\partial v}{\partial x} u\right) = -\frac{\partial P}{\partial y} + \mu_{nf}\left(\frac{\partial^2 v}{\partial y^2} + \frac{\partial^2 v}{\partial x^2}\right)\\ &\quad - \frac{\mu_{nf}}{K} v + g(T - T_c)\rho_{nf}\beta_{nf}\\ &- B_x v B_x \sigma_{nf} + B_x u \sigma_{nf} B_y,\end{aligned} \tag{3}$$

$$(\rho C_p)_{nf}\left(u\frac{\partial T}{\partial x} + \frac{\partial T}{\partial y} v\right) = k_{nf}\left(\frac{\partial^2 T}{\partial x^2} + \frac{\partial^2 T}{\partial y^2}\right) \tag{4}$$

To inform about the amount of properties of nanomaterial components, Ref. [103] can be reviewed. It should be noticed that formulation for nanomaterial is as same as that paper, too. In addition, to gain simpler formulation, pressure terms were discarding by introducing given equation as follows:

$$\begin{aligned}&-\frac{\partial \psi}{\partial x} = v,\\ &\frac{\partial \psi}{\partial y} = u,\\ &\frac{\partial u}{\partial y} - \frac{\partial v}{\partial x} = -\omega,\end{aligned} \tag{5}$$

Considering Eq. (6), the final formulation can be summarized as:

$$\begin{aligned}&\Theta = (q'' L/k_f)^{-1}[T - T],\ V = \frac{vL}{\alpha_f},\\ &(X, Y) = \frac{(x, y)}{L},\ U = \frac{uL}{\alpha_f}\end{aligned} \tag{6}$$

$$\frac{\partial^2 \Psi}{\partial Y^2} + \frac{\partial^2 \Psi}{\partial X^2} = -\Omega \tag{7}$$

$$\left(\frac{\partial^2\Theta}{\partial X^2}+\frac{\partial^2\Theta}{\partial Y^2}\right)=V\frac{\partial\Theta}{\partial Y}+U\frac{\partial\Theta}{\partial X} \tag{8}$$

$$\begin{aligned}&Pr\left(\frac{A_5A_2}{A_1A_4}\right)\left(\frac{\partial^2\Omega}{\partial Y^2}+\frac{\partial^2\Omega}{\partial X^2}\right)+Ra\,Pr\left(\frac{\partial\Theta}{\partial X}\right)\left(\frac{A_3A_2^2}{A_1A_4^2}\right)\\&\quad+Ha^2\,Pr\left[\frac{A_6A_2}{A_1A_4}\right]\left(-\frac{\partial V}{\partial X}(\cos\gamma)^2+(\cos\gamma)\frac{\partial U}{\partial X}(\sin\gamma)\right)\\&\quad-\frac{Pr}{Da}\left(\frac{A_5A_2}{A_1A_4}\right)\Omega\\&\quad+Ha^2\,Pr\left[\frac{A_6A_2}{A_1A_4}\right]\left[-(\sin\gamma)(\cos\gamma)\frac{\partial V}{\partial Y}+\frac{\partial U}{\partial Y}(\sin\gamma)^2\right]\\&\quad=U\frac{\partial\Omega}{\partial X}+\frac{\partial\Omega}{\partial Y}V\end{aligned} \tag{9}$$

$$\begin{aligned}&A_3=\frac{(\rho\beta)_{\mathrm{nf}}}{(\rho\beta)_{\mathrm{f}}},\ A_5=\frac{\mu_{\mathrm{nf}}}{\mu_{\mathrm{f}}},\ Ra=g\beta_{\mathrm{f}}q''L^4/(k_{\mathrm{f}}\upsilon_{\mathrm{f}}\alpha_{\mathrm{f}}),\\&A_2=\frac{(\rho C_{\mathrm{P}})_{\mathrm{nf}}}{(\rho C_{\mathrm{P}})_{\mathrm{f}}},\ Da=\frac{K}{L^2},\\&A_1=\frac{\rho_{\mathrm{nf}}}{\rho_{\mathrm{f}}},\ Pr=\upsilon_{\mathrm{f}}/\alpha_{\mathrm{f}},\\&A_4=\frac{k_{\mathrm{nf}}}{k_{\mathrm{f}}},\ A_6=\frac{\sigma_{\mathrm{nf}}}{\sigma_{\mathrm{f}}},\ Ha=LB_0\sqrt{\sigma_{\mathrm{f}}/\mu_{\mathrm{f}}},\end{aligned} \tag{10}$$

Nu_{loc} and Nu_{ave} and other parameters are determined from:

$$Nu_{\mathrm{loc}}=\frac{1}{\theta}\left(\frac{k_{\mathrm{nf}}}{k_{\mathrm{f}}}\right) \tag{11}$$

Table 1 Variation of outputs with changing mesh when $\phi=0.04,\ Da=100,\ Ha=20$ and $Ra=10^4$

91×271	81×241	71×211	61×181	51×151
2.18871	2.18804	2.18791	2.18783	2.17622

$$Nu_{\mathrm{ave}}=\frac{1}{S}\int_0^s Nu_{\mathrm{loc}}\,\mathrm{d}s \tag{12}$$

$$\begin{aligned}&Be=S_{\mathrm{gen,th}}/S_{\mathrm{gen,total}},\\&S_{\mathrm{gen,total}}=\underbrace{\frac{k_{\mathrm{nf}}}{T^2}\left[\left(\frac{\partial T}{\partial x}\right)^2+\left(\frac{\partial T}{\partial y}\right)^2\right]}_{S_{\mathrm{gen,th}}}\\&\quad+\underbrace{\frac{\mu_{\mathrm{nf}}}{T^2}\left[2\left(\left(\frac{\partial v}{\partial y}\right)^2+\left(\frac{\partial u}{\partial x}\right)^2\right)+\left(\frac{\partial v}{\partial x}+\frac{\partial u}{\partial y}\right)^2\right]}_{S_{\mathrm{gen,f}}}\\&\quad+\underbrace{\frac{\sigma_{\mathrm{nf}}}{T^2}B_0^2v^2}_{S_{\mathrm{gen,M}}}+\underbrace{\frac{\mu_{\mathrm{nf}}}{KT}\left(u^2+v^2\right)}_{S_{\mathrm{gen,P}}}\end{aligned} \tag{13}$$

$$X_{\mathrm{d}}=T_0S_{\mathrm{gen,total}} \tag{14}$$

Results and discussion

This article investigates the nanomaterial irreversibility and thermal behavior through a porous region. Medium with various values of permeability is under the impact of magnetic force. Mesh analysis example is given in Table 1, and validation was performed as shown in Fig. 2 [105]. This graph indicates the good accuracy. Contour plots of various outcomes are demonstrated in Figs. 3, 4, 5 and 6. More fluctuation in contour of magnetic irreversibility can be appeared with the increase in buoyancy effect. This is attributed to domination of convection. Isolines of stream have no significant changes with the increase in Da when Ra has its lowest value. Lorentz forces can increase the resistance against the nanofluid movement, so convective flow reduces. Changing the patterns of isothermal decreases with applying magnetic force, and thermal plume vanishes with augment of Ha. In contrast, exergy drop amount reduces with the increase in Da and Ra. So, to gain

Fig. 2 Outputs of Khanafer et al. [105] versus present data

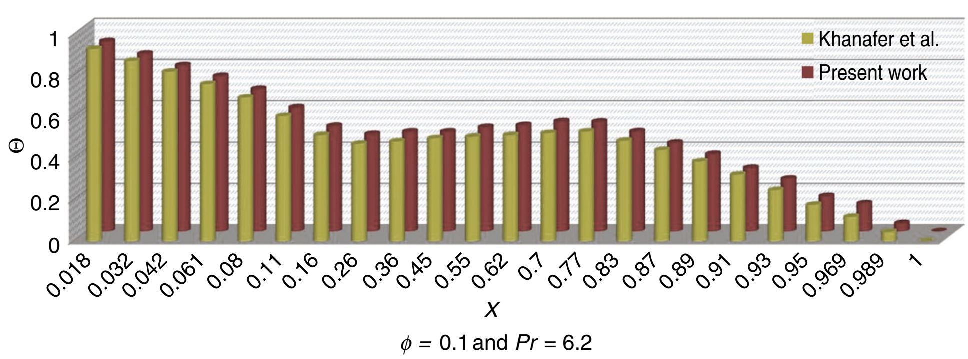

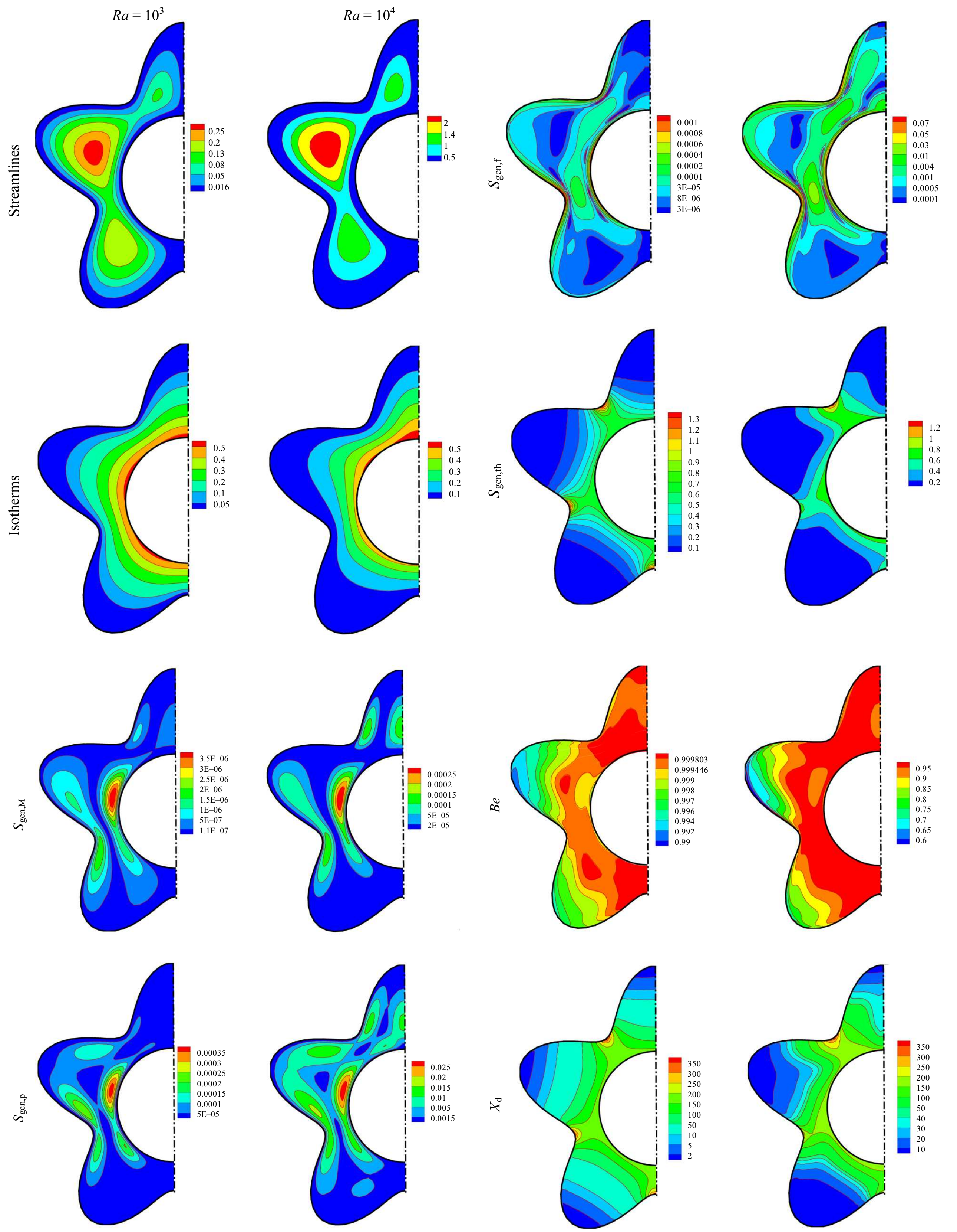

Fig. 3 Impact of buoyancy forces on outcomes at $\phi = 0.04,\ Ha = 1,\ Da = 0.01$

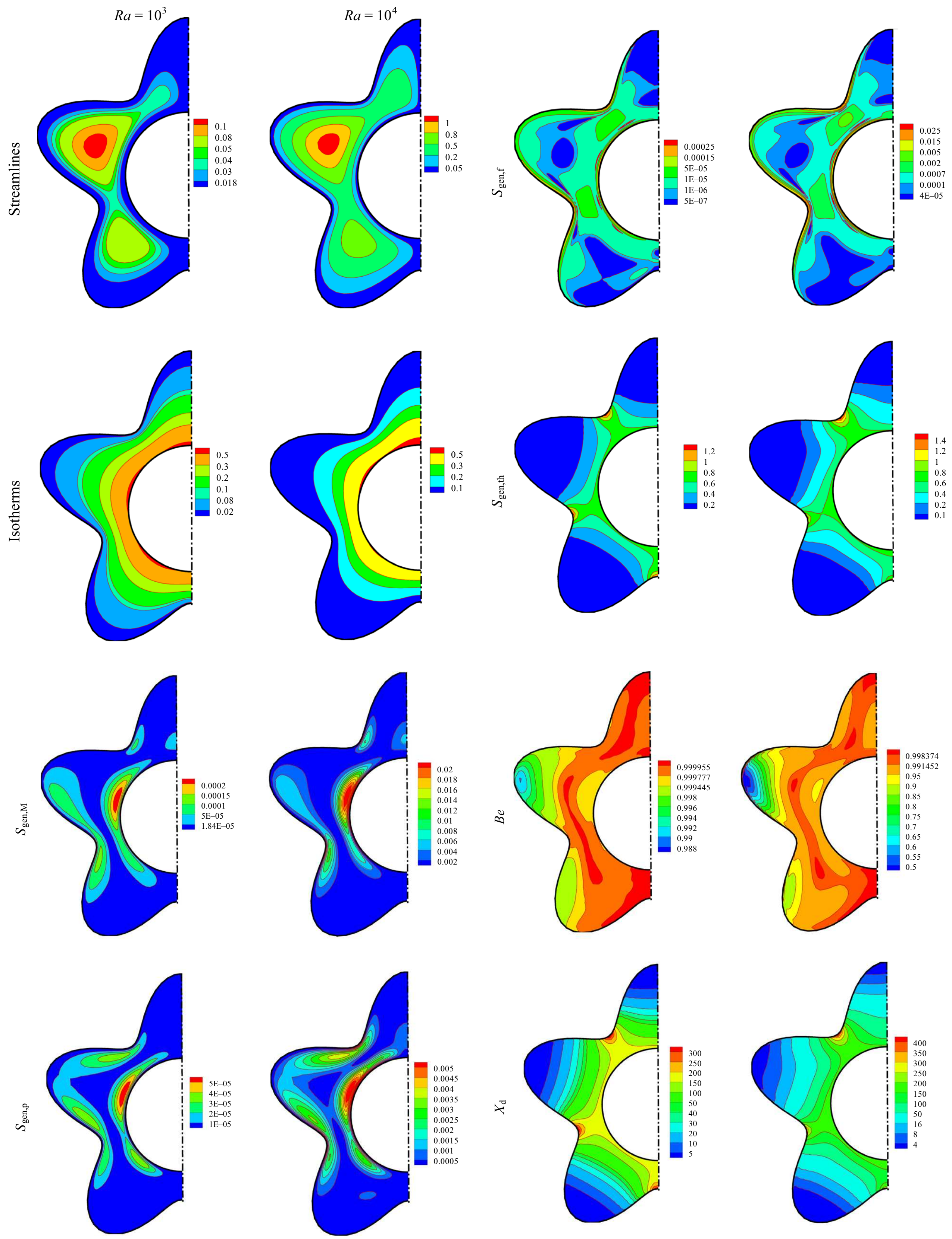

Fig. 4 Impact of buoyancy forces on outcomes at $\phi = 0.04,\ Ha = 20,\ Da = 0.01$

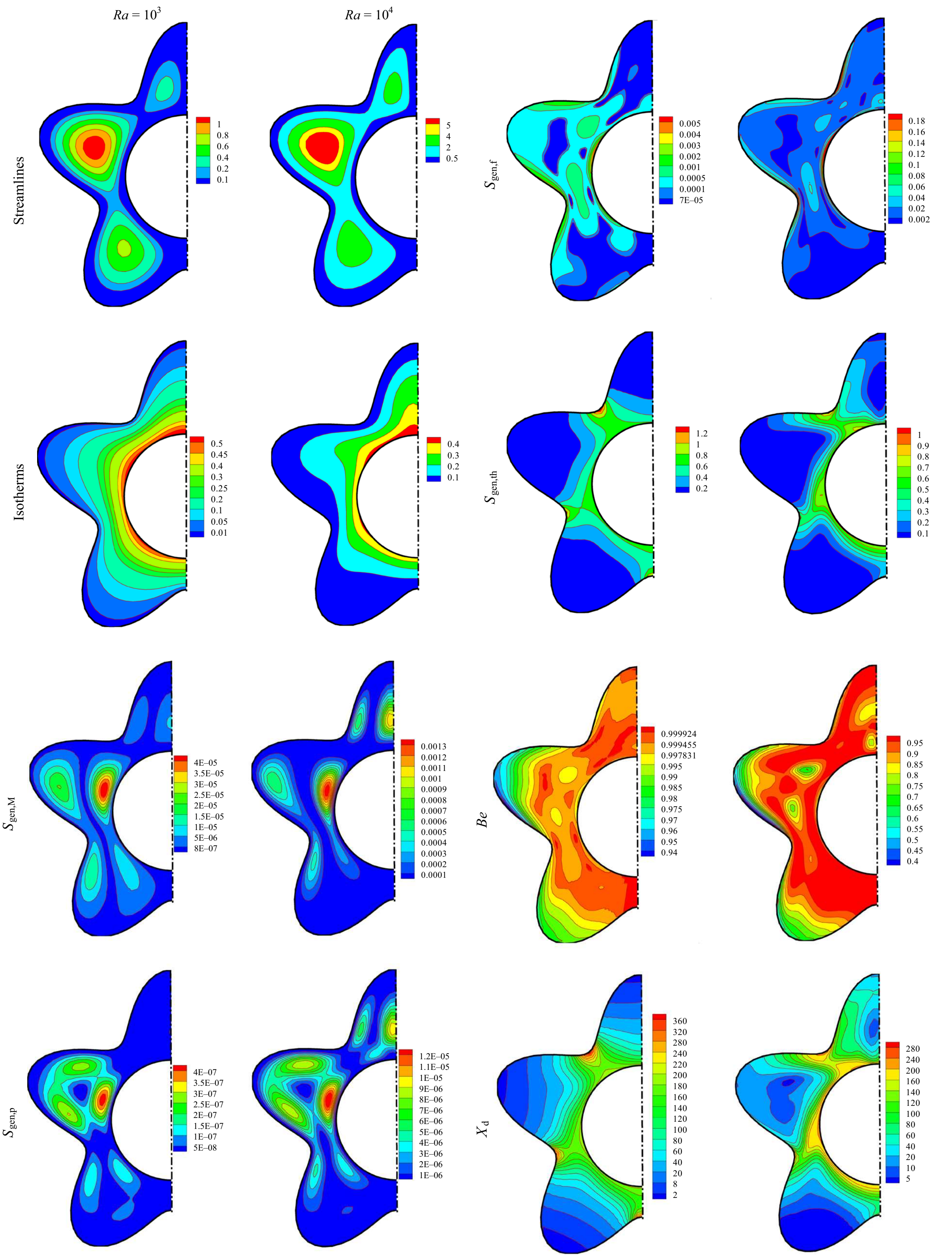

Fig. 5 Impact of buoyancy forces on outcomes at $\phi = 0.04,\ Ha = 1,\ Da = 100$

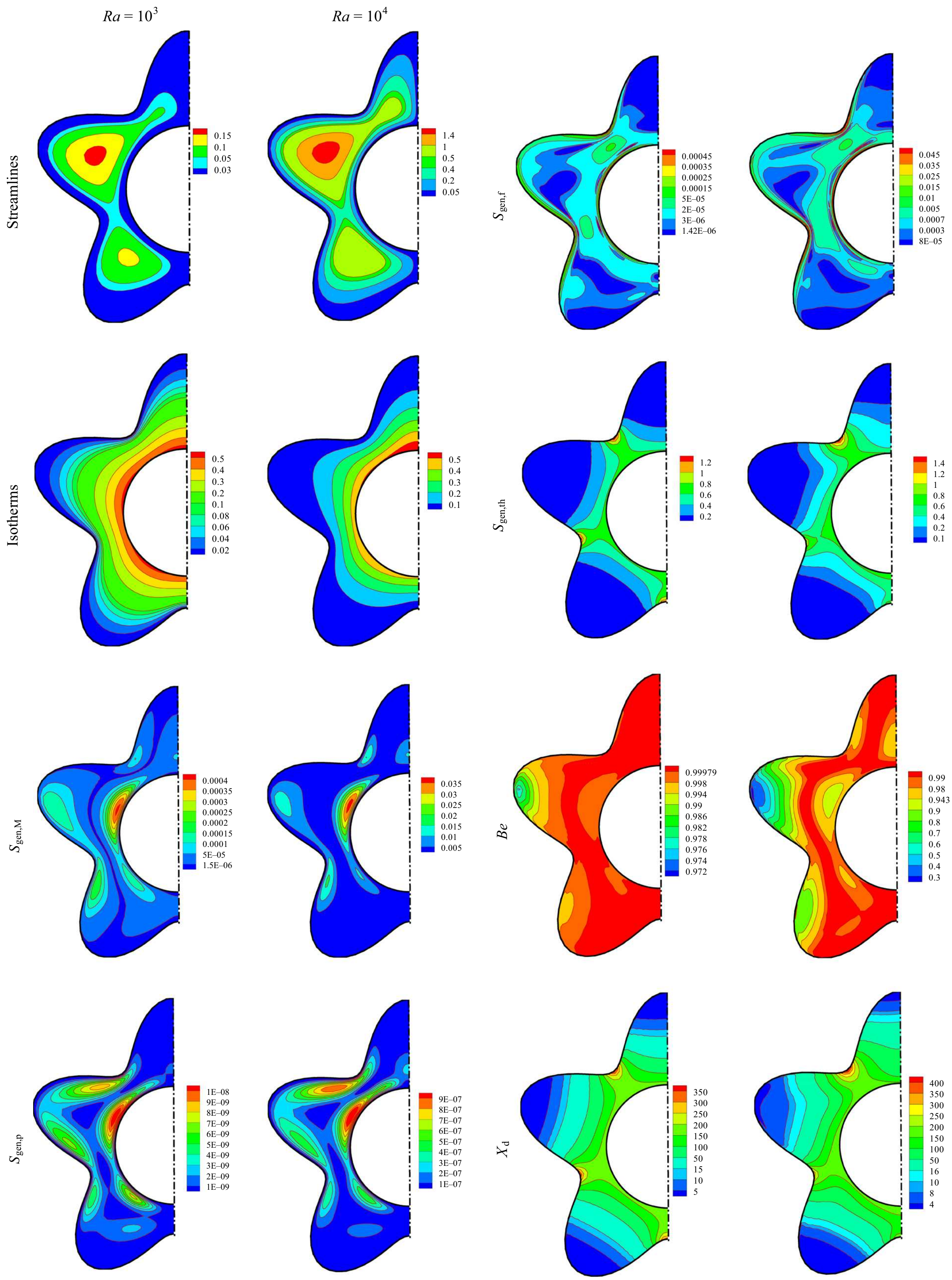

Fig. 6 Impact of buoyancy forces on outcomes at $\phi = 0.04,\ Ha = 20,\ Da = 100$

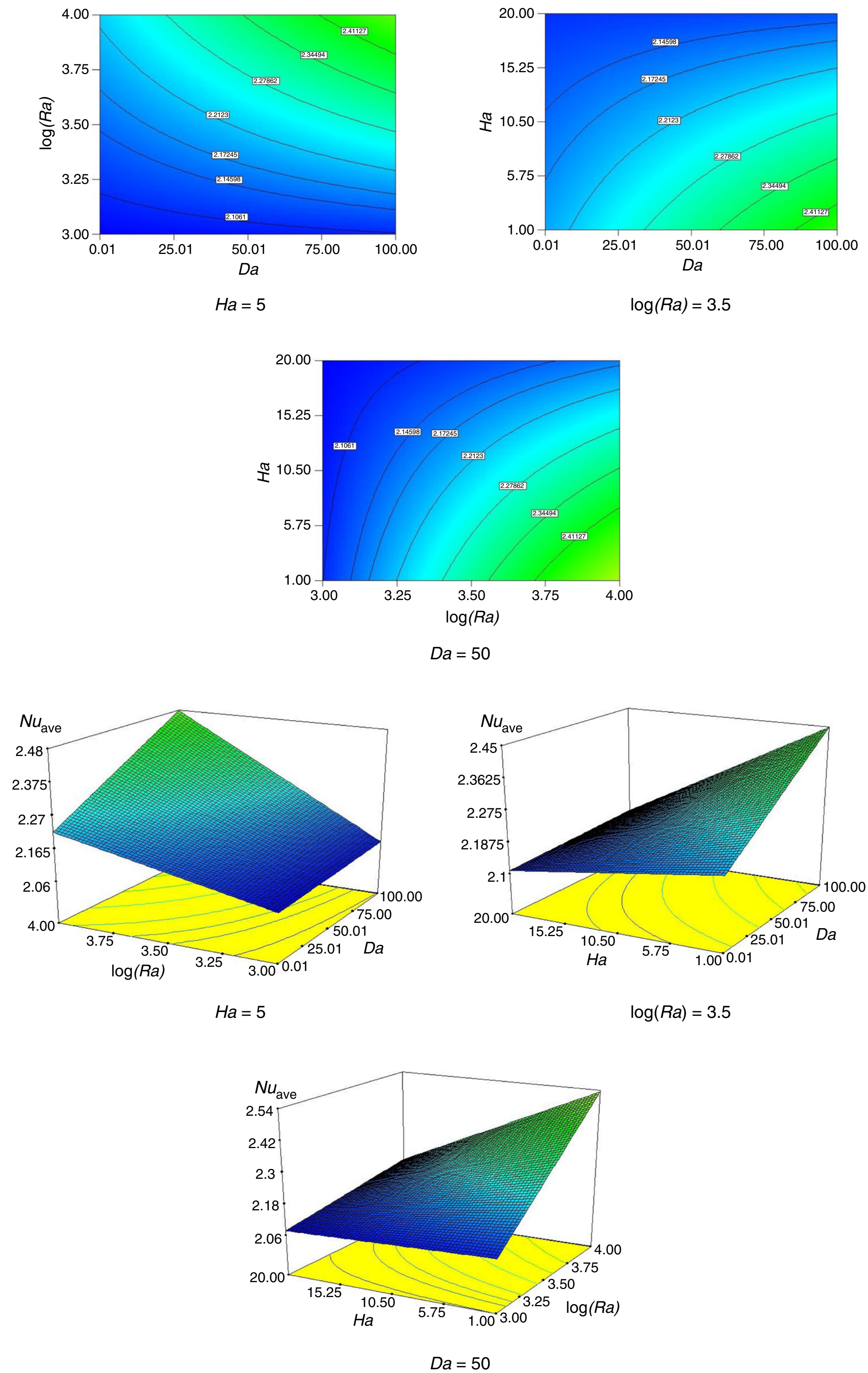

Fig. 7 Various Ra, Ha, Da and obtained Nuave at $\phi = 0.04$

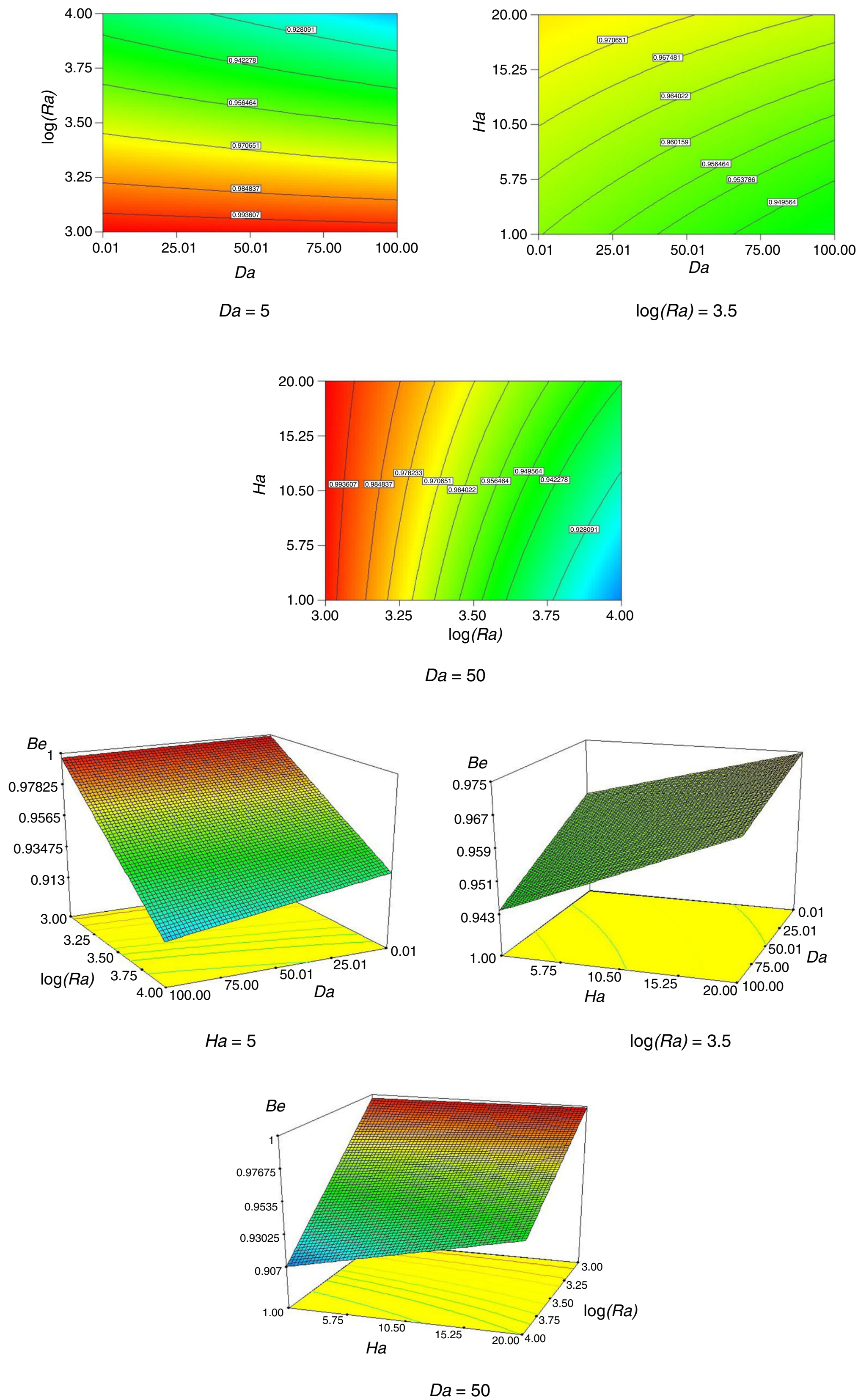

Fig. 8 Various Ra, Ha, Da and obtained Be at $\phi = 0.04$

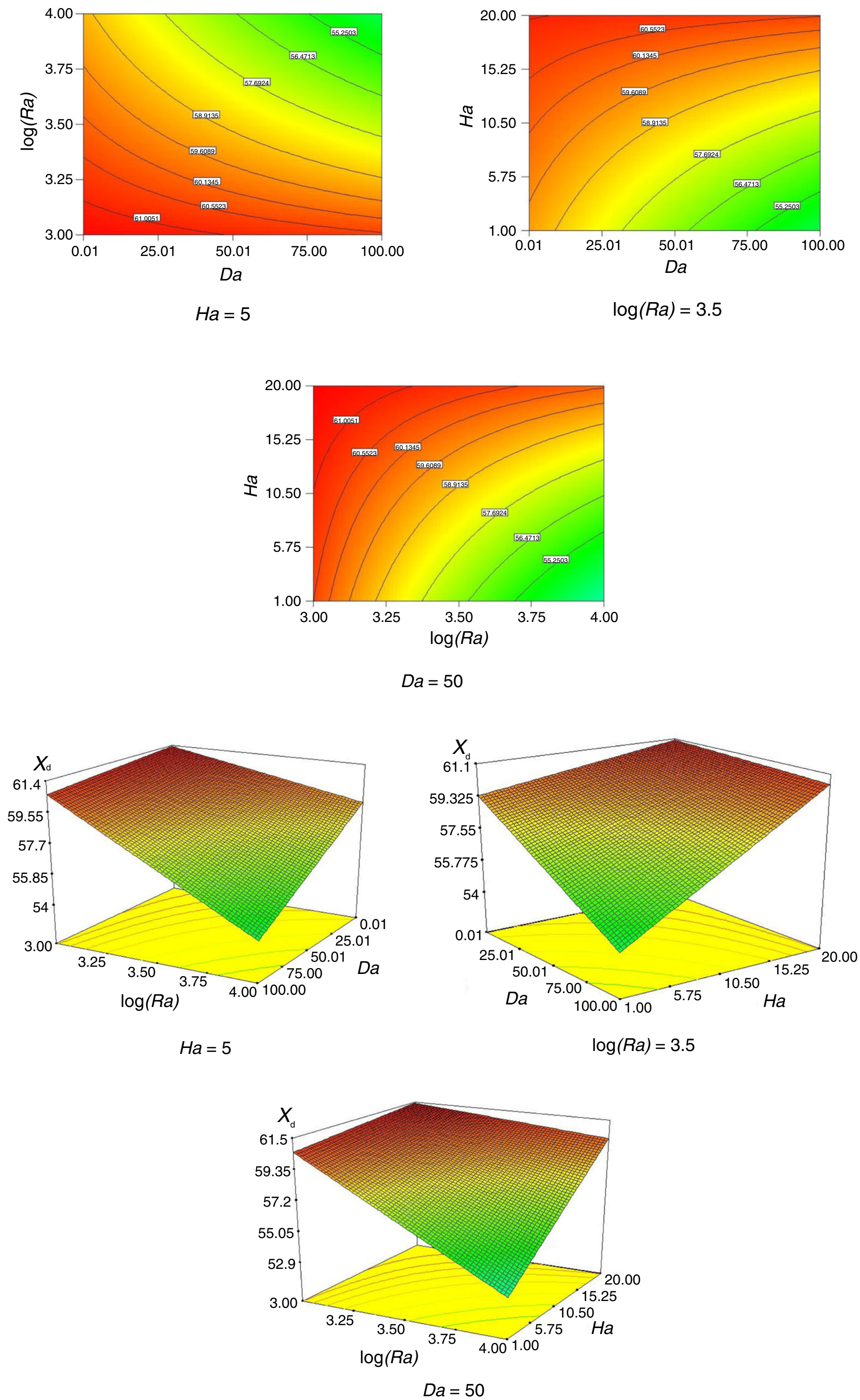

Fig. 9 Various Ra, Ha, Da and obtained X_d at $\phi = 0.04$

the design with minimum irreversibility, lowest values of *Da* and *Ra* should be selected.

Figures 7, 8 and 9 present the changes of the Nu_{ave}, X_d and Bejan number. Feasible way to reach lower exergy drop is selecting greater permeability and stronger buoyancy force. As Da rises, Nu_{ave} improves which can be attributed to reduction in resistance against the nanofluid flow. *Be* increases with augment of Lorenz forces, so to reduce the irreversibility, magnetic effect should be weaken. An augment in permeability of porous region results in augmentation in convective flow and in turn makes Nu_{ave} to increase. It can be determined that X_d and *Ha* have direct relationship. At greater *Da*, changes of exergy drop with *Ha* increase. Permeability has negligible effect on variation of *Be* when buoyancy force is very low. Hartmann number does not expressively affect the Bejan number at low *Ra*. Below formulations belong to above functions:

$$\begin{aligned} Nu_{ave} = 2.22 &+ 0.07Da + 0.13\log(Ra) - 0.099Ha \\ &+ 0.058Da\,\log(Ra) - 0.058Da\,Ha \\ &- 0.085\log(Ra)Ha \end{aligned} \tag{15}$$

$$\begin{aligned} Be = 0.96 &- 0.036\log(Ra) + 8.27\times10^{-3}Ha\log(Ra) \\ &+ 9.34\times10^{-3}Ha - 5.05\times10^{-3}\,\log(Ra)Da \\ &+ 2.12\times10^{-3}Ha\,Da - 6.07\times10^{-3}Da \end{aligned} \tag{16}$$

$$\begin{aligned} X_d = 58.77 &- 1.44Da + 2.22Ha + 1.21Da\,Ha \\ &- 1.08Da\,\log(Ra) - 2.22\log(Ra) + 1.6\log(Ra)Ha \end{aligned} \tag{17}$$

Conclusions

A numerical modeling based on CVFEM was utilized for illustration of nanomaterial movement inside a cavity. Increasing buoyancy force results in greater nanofluid diffusion which guaranteed the higher Nu_{ave}. Permeability augments the power of nanofluid flow which is result in higher Nu_{ave}. Increasing Ha makes the X_d to decline. In contrast, higher values of *Da* result in lower X_d. Exergy loss declines as a consequence of greater buoyancy forces. Augment of the circulation intensity occurs with augment of *Da* while streamlines become weaker with augment of *Ha*.

References

1. Sheikholeslami M, Sheremet MA, Shafee A, Li Z. CVFEM approach for EHD flow of nanofluid through porous medium within a wavy chamber under the impacts of radiation and moving walls. J Therm Anal Calorim. 2019. https://doi.org/10.1007/s10973-019-08235-3.
2. Gao W, Wang WF. The eccentric connectivity polynomial of two classes of nanotubes. Chaos, Solitons Fractals. 2016;89:290–4.
3. Sheikholeslami M. Solidification of NEPCM under the effect of magnetic field in a porous thermal energy storage enclosure using CuO nanoparticles. J Mol Liq. 2018;263:303–15.
4. Gao W, Yan L, Shi L. Generalized Zagreb index of polyomino chains and nanotubes. Optoelectron Adv Mater Rapid Commun. 2017;11(1-2):119–24.
5. Sheikholeslami M, Darzi M, Sadoughi MK. Heat transfer improvement and pressure drop during condensation of refrigerant-based nanofluid; an experimental procedure. Int J Heat Mass Transf. 2018;122:643–50.
6. Sheikholeslami M. Numerical modeling of Nano enhanced PCM solidification in an enclosure with metallic fin. J Mol Liq. 2018;259:424–38.
7. Sheikholeslami M. Numerical simulation for solidification in a LHTESS by means of Nano-enhanced PCM. J Taiwan Inst Chem Eng. 2018;86:25–41.
8. Soomro FA, Zaib A, Haq RU, Sheikholeslami M. Dual nature solution of water functionalized copper nanoparticles along a permeable shrinking cylinder: FDM approach. Int J Heat Mass Transf. 2019;129:1242–9.
9. Sheikholeslami M. Numerical approach for MHD Al2O3-water nanofluid transportation inside a permeable medium using innovative computer method. Comput Methods Appl Mech Eng. 2019;344:306–18.
10. Sheikholeslami M, Barzegar Gerdroodbary M, Moradi R, Shafee A, Li Z. Application of neural network for estimation of heat transfer treatment of Al_2O_3-H_2O nanofluid through a channel. Comput Methods Appl Mech Eng. 2019;344:1–12.
11. Sheikholeslami M, Khan I, Tlili I. Non-equilibrium model for nanofluid free convection inside a porous cavity considering Lorentz forces. Sci Rep. 2018;8:16881. https://doi.org/10.1038/s41598-018-33079-6.
12. Sheikholeslami M. Lattice Boltzmann method simulation of MHD non-Darcy nanofluid free convection. Phys B. 2017;516:55–71.
13. Qin Y. Pavement surface maximum temperature increases linearly with solar absorption and reciprocal thermal inertial. Int J Heat Mass Transf. 2016;97:391–9.
14. Sheikholeslami M, Jafaryar M, Shafee A, Li Z. Hydrothermal and second law behavior for charging of NEPCM in a two dimensional thermal storage unit. Chin J Phys. 2019;58:244–52.
15. Qin Y, Liang J, Tan K, Li F. A side by side comparison of the cooling effect of building blocks with retro-reflective and diffuse-reflective walls. Sol Energy. 2016;133:172–9.
16. Sheikholeslami M, Arabkoohsar A, Khan I, Shafee A, Li Z. Impact of Lorentz forces on Fe_3O_4-water ferrofluid entropy and exergy treatment within a permeable semi annulus. J Clean Prod. 2019;221:885–98.
17. Qin Y, Luo J, Chen Z, Mei G, Yan L-E. Measuring the albedo of limited-extent targets without the aid of known-albedo masks. Sol Energy. 2018;171:971–6.
18. Sheikholeslami M, Jafaryar M, Shafee A, LI Z. Simulation of nanoparticles application for expediting melting of PCM inside a finned enclosure. Phys A. 2019;523:544–56.
19. Qin Y. A review on the development of cool pavements to mitigate urban heat island effect. Renew Sustain Energy Rev. 2015;52:445–59.
20. Sheikholeslami M, Keramati H, Shafee A, Li Z, Alawad OA, Tlili I. Nanofluid MHD forced convection heat transfer around the elliptic obstacle inside a permeable lid drive 3D enclosure

considering lattice Boltzmann method. Phys A: Stat Mech Appl. 2019;523:87–104.
21. Qin Y, He Y, Hiller JE, Mei G. A new water-retaining paver block for reducing runoff and cooling pavement. J Clean Prod. 2018;199:948–56.
22. Sheikholeslami M, Haq R-u, Shafee A, Li Z, Elaraki YG, Tlili I. Heat transfer simulation of heat storage unit with nanoparticles and fins through a heat exchanger. Int J Heat Mass Transf. 2019;135:470–8.
23. Qin Y, Zhao Y, Chen X, Wang L, Li F, Bao T. Moist curing increases the solar reflectance of concrete. Constr Build Mater. 2019;215:114–8.
24. Sheikholeslami M, Shafee A, Zareei A, Haq R-u, Li Z. Heat transfer of magnetic nanoparticles through porous media including exergy analysis. J Mol Liq. 2019;279:719–32.
25. Qin Y, Zhang M, Hiller JE. Theoretical and experimental studies on the daily accumulative heat gain from cool roofs. Energy. 2017;129:138–47.
26. Sheikholeslami M, Mahian O. Enhancement of PCM solidification using inorganic nanoparticles and an external magnetic field with application in energy storage systems. J Clean Prod. 2019;215:963–77.
27. Sheikholeslami M. Magnetic source impact on nanofluid heat transfer using CVFEM. Neural Comput Appl. 2018;30(4):1055–64.
28. Sheikholeslami M, Li Z, Shafee A. Lorentz forces effect on NEPCM heat transfer during solidification in a porous energy storage system. Int J Heat Mass Transf. 2018;127:665–74.
29. Sheikholeslami M, Jafaryar M, Saleem S, Li Z, Shafee A, Jiang Y. Nanofluid heat transfer augmentation and exergy loss inside a pipe equipped with innovative turbulators. Int J Heat Mass Transf. 2018;126:156–63.
30. Sheikholeslami M, Ghasemi A, Li Z, Shafee A, Saleem S. Influence of CuO nanoparticles on heat transfer behavior of PCM in solidification process considering radiative source term. Int J Heat Mass Transf. 2018;126:1252–64.
31. Sheikholeslami M, Shehzad SA, Abbasi FM, Li Z. Nanofluid flow and forced convection heat transfer due to Lorentz forces in a porous lid driven cubic enclosure with hot obstacle. Comput Methods Appl Mech Eng. 2018;338:491–505.
32. Hussien AA, Yusop NM, Abdullah MZ, Al-Nimr MdA, Khavarian M. Study on convective heat transfer and pressure drop of MWCNTs/water nanofluid in mini-tube. J Therm Anal Calorim. 2019;135(1):123–32.
33. Kumar V, Pandya N, Pandya B, Joshi A. Synthesis of metal-based nanofluids and their thermo-hydraulic performance in compact heat exchanger with multi-louvered fins working under laminar conditions. J Therm Anal Calorim. 2019;135(4):2221–35.
34. Wu SY, Wang H, Xiao S, Zhu DS. An investigation of melting/freezing characteristics of nanoparticle-enhanced phase change materials. J Therm Anal Calorim. 2012;110(3):1127–31.
35. Mehrez Z, El Cafsi A. Forced convection magnetohydrodynamic Al_2O_3–Cu/water hybrid nanofluid flow over a backward-facing step. J Therm Anal Calorim. 2019;135(2):1417–27.
36. Sheikholeslami M, Haq R-u, Shafee A, Li Z. Heat transfer behavior of Nanoparticle enhanced PCM solidification through an enclosure with V shaped fins. Int J Heat Mass Transf. 2019;130:1322–42.
37. Rokni HB, Gupta A, Moore JD, McHugh MA, Bamgbaded BA, Gavaises M. Purely predictive method for density, compressibility, and expansivity for hydrocarbon mixtures and diesel and jet fuels up to high temperatures and pressures. Fuel. 2019;236:1377–90.
38. Sheikholeslami M, Zeeshan A, Majeed A. Control volume based finite element simulation of magnetic nanofluid flow and heat transport in non-Darcy medium. J Mol Liq. 2018;268:354–64.
39. Zheng S, Shi Juntai W, Keliu LX. Gas flow behavior through inorganic nanopores in shale considering confinement effect and moisture content. Ind Eng Chem Res. 2018;57:3430–40.
40. Zheng S, Xiangfang L, Juntai S, Tao Z, Dong F, Fengrui S, Chen Yu, Jiucheng D, Liujie L. A semi-analytical model for the relationship between pressure and saturation in the CBM reservoirs. J Nat Gas Sci Eng. 2018;49:365–75.
41. Rokni HB, Moore JD, Gupta A, McHugh MA, Gavaises M. Entropy scaling based viscosity predictions for hydrocarbon mixtures and diesel fuels up to extreme conditions. Fuel. 2019;241:1203–13.
42. Rashidi S, Mahian O, Mohseni LE. Applications of nanofluids in condensing and evaporating systems. J Therm Anal Calorim. 2018;131:2027–39.
43. Jafaryar M, Sheikholeslami M, Li Z, Moradi R. Nanofluid turbulent flow in a pipe under the effect of twisted tape with alternate axis. J Therm Anal Calorim. 2018. https://doi.org/10.1007/s10973-018-7093-2.
44. Sheikholeslami M, Ellahi R. Three dimensional mesoscopic simulation of magnetic field effect on natural convection of nanofluid. Int J Heat Mass Transf. 2015;89:799–808.
45. Sheikholeslami M, Jafaryar M, Li Z. Nanofluid turbulent convective flow in a circular duct with helical turbulators considering CuO nanoparticles. Int J Heat Mass Transf. 2018;124:980–9.
46. Sheikholeslami M. Numerical simulation of magnetic nanofluid natural convection in porous media. Phys Lett A. 2017;381:494–503.
47. Darzi M, Sadoughi MK, Sheikholeslami M. Condensation of nano-refrigerant inside a horizontal tube. Phys B: Condens Matter. 2018;537:33–9.
48. Selvaraj V, Morri B, Nair LM, Krishnan H. Experimental investigation on the thermophysical properties of beryllium oxide-based nanofluid and nano-enhanced phase change material. J Therm Anal Calorim. 2019. https://doi.org/10.1007/s10973-019-08042-w.
49. Sajid MU, Ali HM, Sufyan A, Rashid D, Zahid SU, Rehman WU. Experimental investigation of TiO_2–water nanofluid flow and heat transfer inside wavy mini-channel heat sinks. J Therm Anal Calorim. 2019. https://doi.org/10.1007/s10973-019-08043-9.
50. Sheikholeslami M, Mehryan SAM, Shafee A, Sheremet MA. Variable magnetic forces impact on Magnetizable hybrid nanofluid heat transfer through a circular cavity. J Mol Liq. 2019;277:388–96.
51. Sheikholeslami M, Shah Z, Shafee A, Khan I, Tlili I. Uniform magnetic force impact on water based nanofluid thermal behavior in a porous enclosure with ellipse shaped obstacle. Sci Rep. 2019. https://doi.org/10.1038/s41598-018-37964-y.
52. Dalei J, Jian S. Comparison on the hydraulic and thermal performances of two tree-like channel networks with different size constraints. Int J Heat Mass Transf. 2019;130:1070–4.
53. Farshad SA, Sheikholeslami M. Simulation of nanoparticles second law treatment inside a solar collector considering turbulent flow. Phys A: Stat Mech Appl. 2019;525:1–12.
54. Dalei J, Shiyu S, Lei H. Reexamination of Murray's law for tree-like rectangular microchannel network with constant channel height. Int J Heat Mass Transf. 2019;128:1344–50.
55. Sheikholeslami M, Zareei A, Jafaryar M, Shafee A, Li Z, Smida A, Tlili I. Heat transfer simulation during charging of nanoparticle enhanced PCM within a channel. Phys A: Stat Mech Appl. 2019;525:557–65.

56. Sheikholeslami M, Jafaryar M, Shafee A, Li Z. Analyze of entropy generation for NEPCM melting process inside a heat storage system. Microsyst Technol. 2019. https://doi.org/10.1007/s00542-019-04301-w.
57. Dalei J, Shiyu S, Yunlu P, Xiaoming W. Optimal fractal tree-like microchannel networks with slip for laminar flow-modified Murray's law. Beilstein J Nanotechnol. 2018;9:482–9.
58. Gao W, Guirao JLG, Wu HL. Two tight independent set conditions for fractional (g, f, m)-deleted graphs systems. Qual Theory Dyn Syst. 2018;17(1):231–43.
59. Sheikholeslami M. Influence of magnetic field on Al_2O_3-H_2O nanofluid forced convection heat transfer in a porous lid driven cavity with hot sphere obstacle by means of LBM. J Mol Liq. 2018;263:472–88.
60. Gao W, Wang WF. Degree sum condition for fractional ID-k-factor-critical graphs. Miskolc Math Notes. 2017;18(2):751–8.
61. Dalei J, He L. Thermal characteristics of staggered double-layer microchannel heat sink. Entropy. 2018;20:537.
62. Qin Y, Liang J, Yang H, Deng Z. Gas permeability of pervious concrete and its implications on the application of pervious pavements. Measurement. 2016;78:104–10.
63. Bhatti MM, Sheikholeslami M, Shahid A, Hassan M, Abbas T. Entropy generation on the interaction of nanoparticles over a stretched surface with thermal radiation. Colloids Surf A: Physicochem Eng Asp. 2019;570:368–76.
64. Qin Y. Urban canyon albedo and its implication on the use of reflective cool pavements. Energy Build. 2015;96:86–94.
65. Sheikholeslami M, Jafaryar M, Ali JA, Hamad SM, Divsalar A, Shafee A, Nguyen-Thoi T, Li Z. Simulation of turbulent flow of nanofluid due to existence of new effective turbulator involving entropy generation. J Mol Liq. 2019. https://doi.org/10.1016/j.molliq.2019.111283.
66. Sheikholeslami M, Seyednezhad M. Simulation of nanofluid flow and natural convection in a porous media under the influence of electric field using CVFEM. Int J Heat Mass Transf. 2018;120:772–81.
67. Gao W, Liang L, Chen YH. An isolated toughness condition for graphs to be fractional (k, m)-deleted graphs. Util Math. 2017;105:303–16.
68. Hedayat M, Sheikholeslami M, Shafee A, Nguyen-Thoi T, Henda MB, Tlili I, Li Z. Investigation of nanofluid conduction heat transfer within a triplex tube considering solidification. J Mol Liq. 2019. https://doi.org/10.1016/j.molliq.2019.111232.
69. Dalei J, Lei H, Xiaoming W. Optimization analysis of fractal tree-like microchannel network for electroviscous flow to realize minimum hydraulic resistance. Int J Heat Mass Transf. 2018;125:749–55.
70. Sheikholeslami M, Jafaryar M, Shafee A, Li Z, Haq R-u. Heat transfer of nanoparticles employing innovative turbulator considering entropy generation. Int J Heat Mass Transf. 2019;136:1233–40.
71. Gao W. Three algorithms for graph locally harmonious colouring. J Differ Equ Appl. 2017;23(1–2):8–20.
72. Farshad SA, Sheikholeslami M. FVM modeling of nanofluid forced convection through a solar unit involving MCTT. Int J Mech Sci. 2019;159:126–39.
73. Qin Y, Hiller JE. Understanding pavement-surface energy balance and its implications on cool pavement development. Energy Build. 2014;85:389–99.
74. Qin Y, Zhang M, Mei G. A new simplified method for measuring the permeability characteristics of highly porous media. J Hydrol. 2018;562:725–32.
75. Gao W, Liang L, Xu TW, Zhou JX. Degree conditions for fractional (g, f, n', m)-critical deleted graphs and fractional ID-(g, f, m)-deleted graphs. Bull Malays Math Sci Soc. 2016;39:315–30.
76. Gao W, Wang WF. Toughness and fractional critical deleted graph. Util Math. 2015;98:295–310.
77. Sheikholeslami M. Finite element method for PCM solidification in existence of CuO nanoparticles. J Mol Liq. 2018;265:347–55.
78. Rafatijo H, Monge-Palacios M, Thompson DL. Identifying collisions of various molecularities in molecular dynamics simulations. J Phys Chem A. 2019;123(6):1131–9. https://doi.org/10.1021/acs.jpca.8b11686.
79. Farshad SA, Sheikholeslami M. Nanofluid flow inside a solar collector utilizing twisted tape considering exergy and entropy analysis. Renew Energy. 2019;141:246–58.
80. Gao W. A sufficient condition for a graph to be fractional (a, b, n)-critical deleted graph. Ars Combin. 2015;119:377–90.
81. Sheikholeslami M, Jafaryar M, Hedayat M, Shafee A, Li Z, Nguyen TK, Bakouri M. Heat transfer and turbulent simulation of nanomaterial due to compound turbulator including irreversibility analysis. Int J Heat Mass Transf. 2019;137:1290–300.
82. Gao W, Wang WF. The vertex version of weighted wiener number for bicyclic molecular structures. Comput Math Methods Med, vol. 2015, Article ID 418106, 10 pages. http://dx.doi.org/10.1155/2015/418106.
83. Rafatijo H, Thompson DL. General application of Tolman's concept of activation energy. J Chem Phys. 2017;147:224111. https://doi.org/10.1063/1.5009751.
84. Sheikholeslami M, Ghasemi A. Solidification heat transfer of nanofluid in existence of thermal radiation by means of FEM. Int J Heat Mass Transf. 2018;123:418–31.
85. Gao W, Wang WF. Second atom-bond connectivity index of special chemical molecular structures. J Chem, vol. 2014, Article ID 906254, 8 pages. http://dx.doi.org/10.1155/2014/906254.
86. Sheikholeslami M, Zeeshan A. Analysis of flow and heat transfer in water based nanofluid due to magnetic field in a porous enclosure with constant heat flux using CVFEM. Comput Methods Appl Mech Eng. 2017;320:68–81.
87. Sheikholeslami M, Vajravelu K. Nanofluid flow and heat transfer in a cavity with variable magnetic field. Appl Math Comput. 2017;298:272–82.
88. Sheikholeslami M, Shamlooei M. Fe_3O_4–H_2O nanofluid natural convection in presence of thermal radiation. Int J Hydrog Energy. 2017;42(9):5708–18.
89. Sheikholeslami M, Shehzad SA, Li Z, Shafee A. Numerical modeling for Alumina nanofluid magnetohydrodynamic convective heat transfer in a permeable medium using Darcy law. Int J Heat Mass Transf. 2018;127:614–22.
90. Alkanhal TA, Sheikholeslami M, Arabkoohsar A, Haq R-u, Shafee A, Li Z, Tlili I. Simulation of convection heat transfer of magnetic nanoparticles including entropy generation using CVFEM. Int J Heat Mass Transf. 2019;136:146–56.
91. Sheikholeslami M, Rokni HB. Melting heat transfer influence on nanofluid flow inside a cavity in existence of magnetic field. Int J Heat Mass Transf. 2017;114:517–26.
92. Sheikholeslami M, Rokni HB. Magnetic nanofluid flow and convective heat transfer in a porous cavity considering Brownian motion effects. Phys Fluids. 2018. https://doi.org/10.1063/1.5012517.
93. Sheikholeslami M, Shehzad SA. CVFEM for influence of external magnetic source on Fe_3O_4–H_2O nanofluid behavior in a permeable cavity considering shape effect. Int J Heat Mass Transf. 2017;115:180–91.
94. Sheikholeslami M. Magnetic field influence on CuO–H_2O nanofluid convective flow in a permeable cavity considering various shapes for nanoparticles. Int J Hydrog Energy. 2017;42:19611–21.

95. Sheikholeslami M, Shehzad SA. CVFEM simulation for nanofluid migration in a porous medium using Darcy model. Int J Heat Mass Transf. 2018;122:1264–71.
96. Sheikholeslami M, Hayat T, Alsaedi A, Abelman S. Numerical analysis of EHD nanofluid force convective heat transfer considering electric field dependent viscosity. Int J Heat Mass Transf. 2017;108:2558–65.
97. Alkanhal TA, Sheikholeslami M, Usman M, Haq R-u, Shafee A, Al-Ahmadi AS, Tlili I. Thermal management of MHD nanofluid within the porous medium enclosed in a wavy shaped cavity with square obstacle in the presence of radiation heat source. Int J Heat Mass Transf. 2019;139:87–94.
98. Sheikholeslami M, Rokni HB. Influence of EFD viscosity on nanofluid forced convection in a cavity with sinusoidal wall. J Mol Liq. 2017;232:390–5.
99. Sheikholeslami M. Application of Darcy law for nanofluid flow in a porous cavity under the impact of Lorentz forces. J Mol Liq. 2018;266:495–503.
100. Sheikholeslami M, Seyednezhad M. Nanofluid heat transfer in a permeable enclosure in presence of variable magnetic field by means of CVFEM. Int J Heat Mass Transf. 2017;114:1169–80.
101. Selimefendigil F, Oztop HF, Abu-Hamdeh NH. Mixed convection due to a rotating cylinder in a 3D corrugated cavity filled with single walled CNT-water nanofluid. J Therm Anal Calorim. 2019;135:341–55.
102. Bellos E, Tzivanidis C. Thermal efficiency enhancement of nanofluid-based parabolic trough collectors. J Therm Anal Calorim. 2019;135(1):597–608.
103. Sheikholeslami M. New computational approach for exergy and entropy analysis of nanofluid under the impact of Lorentz force through a porous media. Comput Methods Appl Mech Eng. 2019;344:319–33.
104. Sheikholeslami M. Application of control volume based finite element method (CVFEM) for nanofluid flow and heat transfer. Amsterdam: Elsevier; 2019. ISBN: 9780128141526.
105. Khanafer K, Vafai K, Lightstone M. Buoyancy-driven heat transfer enhancement in a two-dimensional enclosure utilizing nanofluids. Int J Heat Mass Transf. 2003;46:3639–53.